

Doubling the Rate of Spectrally Efficient FDM Systems Using Hilbert Pulse Pairs

Xinyue Liu and Izzat Darwazeh
Department of Electrical and Electronics Engineering
University College London
London, United Kingdom
E-Mail: x.liu.17@ucl.ac.uk, i.darwazeh@ucl.ac.uk

Abstract—This paper proposes a new multi-carrier signal format for spectrally efficient frequency division multiplexing (SEFDM) system to further improve the spectral efficiency, where a Hilbert pair is utilised as pulse-shaping filters. In this work, the square-root raised cosine (SRRC) pulse is employed to generate the Hilbert pulse pair at the transmitter and an equivalent matched filter configuration is used to generate the receiver Hilbert pair. To verify the data rate gain of the proposed system, we generate the mathematical models and carry out simulations with varying compression factor of the SEFDM signals. The numerical modelling results show that the proposed system doubles the data rate relative to conventional SEFDM system with no bit error rate (BER) performance degradation. In addition, results are reported for un-coded transmission and also for system using turbo coding, showing significant BER improvement.

Index Terms—SEFDM, Hilbert pair, turbo coding, data rate, spectral efficiency

I. INTRODUCTION

As 5G approaches, the need for wireless capacity due to the ever increasing number of connected devices and their increasing usage, places an exponentially growing demand for high data rate and low spectral usage communication systems. The scarcity of available spectrum largely drives this demand, and as such, spectral efficiency is a key performance metric for evaluation [1]. Among modern communication techniques, multicarrier modulation (MCM) is commonly-used, due to its robustness against multipath channel impairments. The most popular type of MCM is orthogonal frequency division multiplexing (OFDM), which consists of N subcarriers spaced at $1/T$ intervals, where T is the period of symbols modulating each of the subcarriers, leading to the subcarrier orthogonality [2]. This orthogonal subcarrier spacing prevents inter-carrier interference (ICI). OFDM has been widely adopted in numerous wireless systems and standards, such as 4G-LTE and 802.11a/g [2]. OFDM is capable of optimising the spectral efficiency by using adaptive bit- and power-loading [3] [4]. However, it must maintain the $1/T$ subcarrier spacing, and hence, for a given modulation, no further improvement in spectral efficiency may be obtained.

In order to further improve spectral utilisation, recent research focus has shifted to non-orthogonal multicarrier signals, such as those based on faster-than-Nyquist (FTN) signalling [5], which was a baseband pulse-based format firstly proposed

by Mazo in 1975 [6]. FTN violates the Nyquist criteria by increasing the signalling rate up to 25% without degradation to the BER performance, despite self-induced inter-symbol interference (ISI). The basic concept of non-orthogonality was later adopted and extended to an MCM format [5], hence offering a direct use of FTN in practical multicarrier signalling. The main problem of FTN is in its practical implementation part. Since FTN transmits at a higher information rate relative to its orthogonal counterpart, sophisticated detection algorithms are required at the receiver. Therefore, increased detector complexity constrains hardware implementation due to additional digital signal processing (DSP) requirements.

Another technique used to generate non-orthogonal signals is spectrally efficient frequency division multiplexing (SEFDM), initially proposed by Rodrigues and Darwazeh in 2003 [7]. Ever since, this technique has been developed theoretically and practically covering various topics and these are generally described in [8]. SEFDM purposely violates the orthogonality between subcarriers by compressing frequency spacing between adjacent subcarriers below $1/T$. Analogously to FTN, where ISI is introduced by interference between adjacent pulses, ICI is introduced in SEFDM subcarriers. Similarly, the enhancement of bandwidth efficiency and capacity [9] is traded against the cost of the self-introduced ICI, which is performance degradation and detection complexity.

Although OFDM is now chosen for 5G standards, Several modulation schemes have been considered [10]. Candidates such as filter bank multi-carrier (FBMC), generalized frequency division multiplexing (GFDM) and universal filtered multi-carrier (UFMC) use non-OFDM signalling to improve spectral efficiency [11]. These techniques employ pulse shaping filters in different methods and consequently suppress the out-of-band (OOB) emission of the generated spectrum. Nevertheless, all these techniques suffer from the high complexity of the transmitter and/or the receiver as well as the uncertain feasibility of corresponding hardware implementation.

Advantageously, signals can be generated using a Hilbert pair, which is a pair of pulse shapes that generate orthogonal signals as has been recently utilised in optical carrier-less amplitude and phase Modulation (CAP) [12]. In this work, we propose to couple the Hilbert pair with a SEFDM to improve further bandwidth efficiency relative to conventional SEFDM systems. This is accomplished by splitting the input

symbols into two streams and modulating two sets of subcarriers, occupying the same baseband spectral range. Then, the baseband complex modulated subcarriers are linearly added to give two output streams. For these streams, Pulse shaping and modulation/demodulation by a Hilbert pair guarantees an added level of orthogonality and consequently no interference when separating and decoding a signal comprising two streams occupying the same bandwidth. This results in doubling the spectral efficiency and importantly without incurring power penalty. The price to pay, however, is the increased transceiver complexities. For Hilbert pair pulse shaping, we employ a root-Nyquist pulse shape; specifically the square root raised cosine (SRRC) pulse with a matched filter at the receiver. We verify the results using raw data transmission as well as Turbo coding.

The paper is organised as follows; Section II briefly presents the principal model of SEFDM signal and Hilbert pulse pair. Section III states the modelling methodology followed by a description of system characteristics. In section IV, we evaluate the proposed system performance with respect to the spectral efficiency and BER, with the comparison of different compression factors and the consideration of turbo coding. Finally, conclusions are drawn in section V.

II. SYSTEM MODEL

A. SEFDM Signals

The discrete-time representation for the k^{th} time sample of a single SEFDM symbol may be expressed as [13]:

$$X[k] = \frac{1}{\sqrt{Q}} \sum_{n=0}^{N-1} s_n \cdot e^{j2\pi nk\alpha/Q}, \quad (1)$$

where $\mathbf{s} = [s_0, s_1, \dots, s_{N-1}]$ is the incoming M-ary quadrature amplitude modulation (M-QAM) signal vector for N subcarriers and Q represents the total number of discrete-time samples in one SEFDM symbol. Given that the number of samples-per-symbol is denoted by ρ , there are $Q = \rho N$ ($\rho \geq 1, \rho \in \mathbb{Z}$) samples for the discrete time SEFDM scheme. The factor $1/\sqrt{Q}$ is for the purpose of normalisation. Importantly, OFDM and SEFDM are differentiated by the bandwidth compression factor ($\alpha = 1$ for OFDM and < 1 for SEFDM), which determines the bandwidth saving in comparison to OFDM by $(1 - \alpha) \times 100\%$.

B. The Hilbert Pairs

The Hilbert pair originates from the in-phase (I) and quadrature (Q) components of the analytic signal $f_+(t)$ given by [14]:

$$f_+(t) = f(t) + j \cdot \hat{f}(t), \quad (2)$$

wherein $f(t)$ is a real-valued function with continuous value t . Its Hilbert transform $\hat{f}(t)$ can be expressed using either an integration or a convolution as [14]:

$$\hat{f}(t) = \mathcal{H}\{f(t)\} = f(t) * \frac{1}{\pi t} = \frac{1}{\pi} P \int_{-\infty}^{+\infty} \frac{f(\tau)}{t - \tau} d\tau, \quad (3)$$

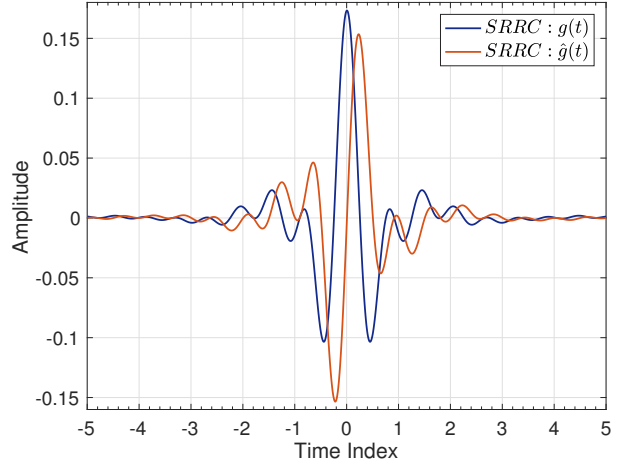


Fig. 1. Time domain representation of the Hilbert pair formed by SRRC pulse ($\beta = 0.35$)

where $\mathcal{H}[\cdot]$ is the Hilbert transform operator. It is worth stating that the real function $f(t)$ and its Hilbert Transform $\hat{f}(t)$ are orthogonal:

$$\int_{-\infty}^{+\infty} f(t) \cdot \hat{f}(t) dt = 0. \quad (4)$$

To construct the orthogonal filter pair $g(t)$ and $\hat{g}(t)$, we multiply a given pulse shape $p(t)$ with a Hilbert pair $f(t)$ and $\hat{f}(t)$, as is shown in the equation below [15]:

$$g(t) = p(t)f(t), \quad \hat{g}(t) = p(t)\hat{f}(t). \quad (5)$$

Traditionally, a pair of sinusoidal carrier and co-sinusoidal carriers are used to form the Hilbert pair. Subsequently, the impulse response of the shaping pulse filters are the product of the pulse $p(t)$ and the carrier pair of frequency f_c , given by [12]:

$$g(t) = p(t)\cos(2\pi f_c t), \quad \hat{g}(t) = p(t)\sin(2\pi f_c t). \quad (6)$$

In this work, we employ SRRC pulse, a commonly-used root-Nyquist pulse, as the shape function $p(t)$ of the filter pair. It is assumed that the corresponding matched receiver is used in the system. The SRRC pulse is expressed by:

$$p(t) = \frac{2\beta \left[\cos\left(\frac{(1+\beta)\pi t}{T_s}\right) + \sin\left(\frac{(1-\beta)\pi t}{T_s}\right) \left(\frac{4\beta t}{T_s}\right)^{-1} \right]}{\pi \sqrt{T_s} \left[1 - \left(\frac{4\beta t}{T_s}\right)^2 \right]}, \quad (7)$$

where the roll-off factor $\beta \in [0, 1]$ controls the excess bandwidth, T_s represents the symbol period. The filter bandwidth is equal to $B = (1 + \beta)/2T_s$. Fig.1 depicts the time-domain representation of the aforementioned filter pair generated by SRRC pulse with $\beta = 0.35$.

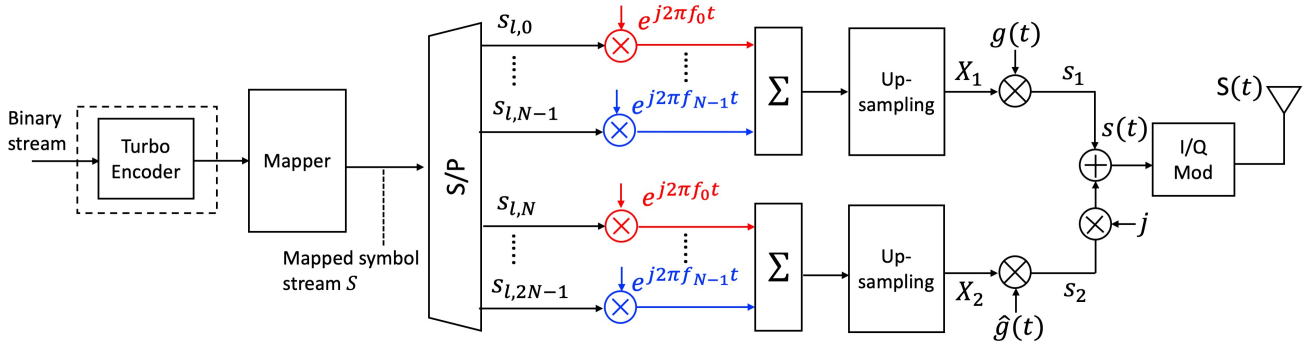


Fig. 2. Simplified transmitter block diagram: $g(t)$ and $\hat{g}(t)$ are from equation (6); the portions in the same colour (red and blue) represent the same subcarriers

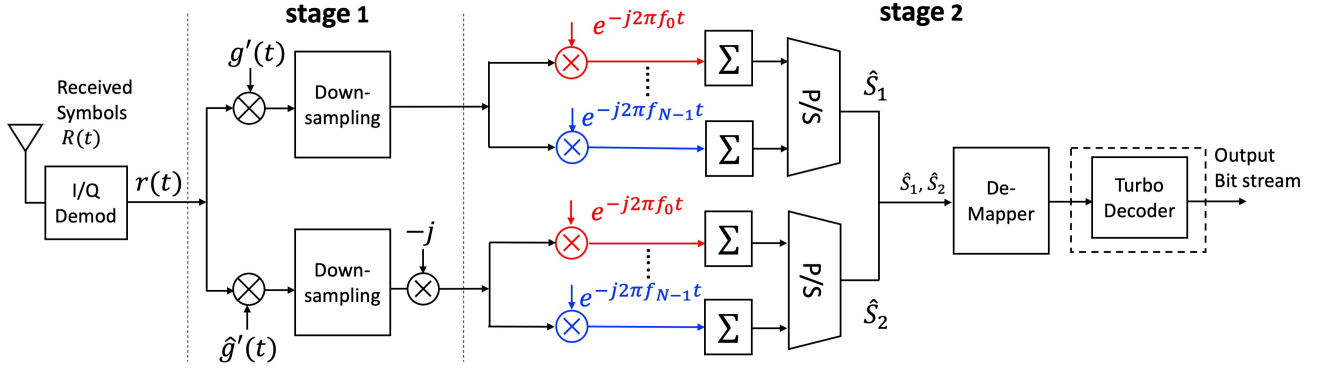


Fig. 3. Simplified receiver block diagram: $g'(t)$ and $\hat{g}'(t)$ are from equation (10); the portions in the same colour (red and blue) represent the same subcarriers

III. MODULATION AND DEMODULATION SCHEME

A. Modulation Scheme

Figure 2 depicts the block diagram of the transmitter of the proposed system. The incoming binary data stream is mapped either un-coded or with turbo coding of rate $(1/3)$. Assuming M -QAM modulation, $2N$ complex symbols $\mathbf{S} = [s_{l,0}, s_{l,1}, \dots, s_{l,2N-1}]$ are generated, where l represents the time sample index. Specifically, 4-QAM modulation scheme is used in the mapper block shown in Fig. 2, indicating that complex symbols are generated with I and Q components. The symbol stream is then split into two blocks of $N = 16$ parallel lower-rate sub-streams vectorised as $\mathbf{S}_1 = [s_{l,0}, \dots, s_{l,N-1}]$ and $\mathbf{S}_2 = [s_{l,N}, \dots, s_{l,2N-1}]$.

For simplicity, a bank of modulators is used here to generate the SEFDM carriers with different compression levels ($\alpha = 0.6, 0.8, 1$) that are used for both of the separate and independent frames. Thus, \mathbf{S}_1 and \mathbf{S}_2 are modulated onto the same subcarrier frequencies and will be later separated in phase by the Hilbert pair. Before pulse shaping, both groups of signals are up-sampled via zero-padding between successive samples with the upsampling factor $q = 4$.

Let \mathbf{X}_1 and \mathbf{X}_2 be the up-sampled SEFDM signal on the two independent frames, and hence the process of pulse shaping can be expressed as:

$$s_1(t) = g(t) * \mathbf{X}_1, \quad s_2(t) = \hat{g}(t) * \mathbf{X}_2, \quad (8)$$

where $g(t)$ and $\hat{g}(t)$ are a normalised Hilbert pulse pair yielded from (6). The filters have 10 symbols length span since ideal filters of infinite length are impractical. The outputs of the two orthogonal filters are added up, after multiplying the second stream by j to give $s(t)$, which can be expressed by

$$s(t) = s_1(t) + j \cdot s_2(t). \quad (9)$$

The achieved signal is then converted to RF signal by I/Q modulation and passed through the wireless channel, which, for this work is assumed to be a simple additive white Gaussian noise (AWGN) channel.

B. Demodulation and Recovery

Figure 3 shows the block diagram of the receiver, which functionally incorporates two stages; the first separates two symbol streams and demodulates the signal in each. The second stage employs time-reversed matched filtering (MF) without the use of advanced detection methods. The matched filtering pair at the first stage can be obtained by flipping the Hilbert pulse pair in the time domain, as given by [12]:

$$g'(t) = g(-t), \quad \hat{g}'(t) = \hat{g}(-t). \quad (10)$$

The matched pair $g'(t)$ and $\hat{g}'(t)$ separate the received signals into two sub-streams followed by the downsampling and decimation process. On the second frame $-j$ is introduced with the negative sign to recover the signal as in the lower

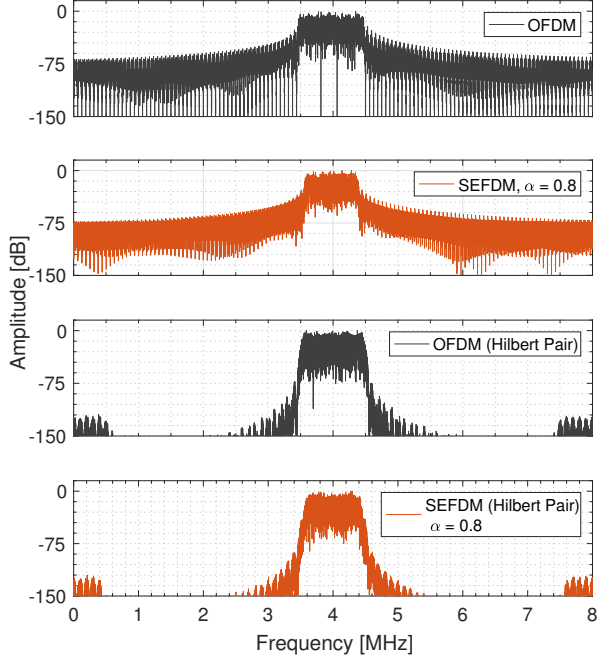


Fig. 4. Spectrum Comparison: OFDM; SEFDM ($\alpha = 0.8$); OFDM using Hilbert pulse pair; SEFDM using Hilbert pulse pair ($\alpha = 0.8$). $N = 16$ for all cases.

arm of transmitter. Once two groups of symbols are properly separated, matched filtering along with hard decision work in the manner as in conventional SEFDM or OFDM systems. The matched filtering at the second stage is equivalent to the conjugate complex of the subcarriers matrix Φ^* . The demodulation process can be expressed as [13]

$$\hat{S} = \Phi^* R = \Phi^* (X + W) = \Phi^* \Phi S + \Phi^* W, \quad (11)$$

where \hat{S} represents the demodulated signal, Φ is the Q -by- N subcarrier matrix, Φ^* is an N -by- Q matrix, the input X is defined by (1) and W denotes the noise vector. The correlation matrix C is constructed as [13]:

$$C = \Phi^* \Phi, \quad (12)$$

where ideally the correlation denotes an N -by- N unitary matrix, and consequently the received signals can be recovered if the introduced noise-associated term can be removed or suppressed. As is shown in the equation, the AWGN noise is expanded by the complex conjugate of the subcarrier matrix. Since we use the orthogonal Hilbert pair, no degradation is introduced to the correlation matrix C , the proposed system is expected to have an identical BER performance when compared to the conventional SEFDM.

The recovered complex symbol streams, termed as \hat{S}_1 and \hat{S}_2 are input into the demapper block serially. When turbo coding is used, based on the investigation in [16], 5 iterations are optimal to counteract the introduced ICI of SEFDM. A soft de-mapper is then used with the log-likelihood ratio (LLR)

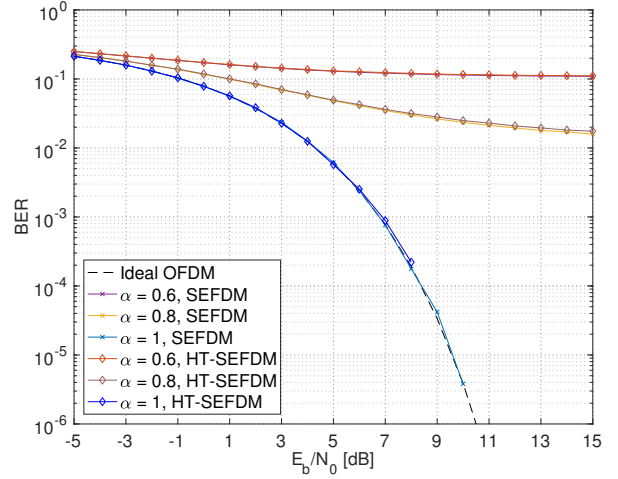


Fig. 5. BER performance comparison of SEFDM signals with and without pulse-shaping using Hilbert SRRC pair ($\alpha = 0.6, 0.8, 1, \beta = 0.35$)

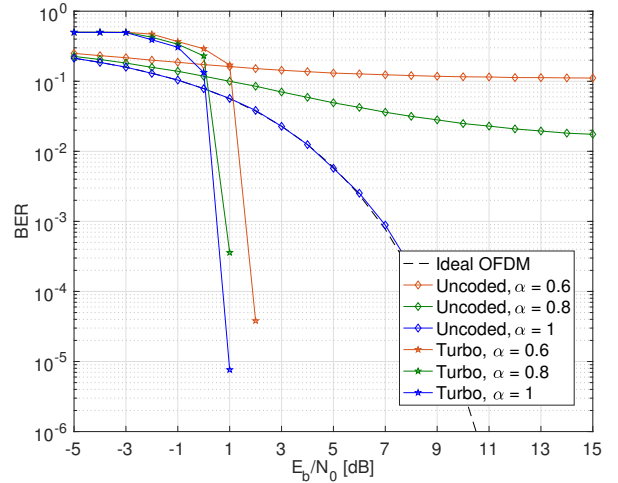


Fig. 6. BER performance of SEFDM signals pulse-shaped by Hilbert SRRC pair with and without turbo Coding ($\alpha = 0.6, 0.8, 1, \beta = 0.35$)

algorithm so that soft bit and extrinsic information (from the previous iteration) are utilised to feed the turbo decoder.

IV. PERFORMANCE INVESTIGATIONS

We assess the proposed system performance by studying the BER for different α values. Tests are carried out on both conventional SEFDM and the proposed system for the purpose of comparison. The mathematical models are designed and generated in MATLAB.

A. Spectral Efficiency Property

Figure 4 compares the normalised spectrum of the conventional SEFDM signal and the proposed transmitted signal when the compression factor α is equal to 0.8 and 1 (OFDM). It is known that the inherent non-orthogonality of SEFDM signal, leading to the compression of the frequency spacing

between adjacent subcarriers, results in the spectral efficiency gain when compared to OFDM signal. The spectral efficiency generally describes the maximum data rate R_b that can be transmitted over a particular bandwidth B and hence can be measured by their ratio. Therefore, the smaller α is, the higher the spectral efficiency that can be achieved due to the decreased bandwidth consumption. Figure 4 shows that the designed signal filtered by the Hilbert pair occupies the same bandwidth at the same carrier frequency as compared to the SEFDM. In conventional SEFDM, the frequency spectrum carries only one symbol stream. However, with the same spectrum utilisation the frequency spectrum of the proposed signal carries two independent 4-QAM symbol streams, leading to a doubled data rate. Consequently, the spectral efficiency of the proposed signal can be expressed as $2\log_2 MR_s/\alpha B$ bits/s/Hz, which is twice the spectral efficiency of the SEFDM (i.e. $\log_2 MR_s/\alpha B$ bits/s/Hz) when using the same α . This leads to the conclusion that by using the Hilbert pulse pair, the spectral efficiency is doubled.

B. BER Performance

The BER performance of the proposed system using Hilbert pulse pair is investigated in terms of different choices of the compression factor α . Given that the SEFDM system is ill-conditioned when $\alpha \leq 0.8$ when only MF is used, the system will not be expected to lead to good BER results. To improve performance, turbo coding is added and at the receiver the decoder employs 5 iterations based on the results obtained in [16]. This is to confirm that coding is effective in enhancing the BER of the proposed system.

Figure 5 demonstrates the BER performance of the signal generated from the proposed design given in Fig. 2 versus E_b/N_0 . It is evident that the proposed system achieves identical BER performance compared to the conventional OFDM ($\alpha = 1$) and SEFDM ($\alpha = 0.8, 0.6$). With the reduction of the compression factor α , the error performance degrades rapidly, which is in accordance with the theoretical results. This leads to the conclusion that the use of Hilbert pulse pair as shaping pulses doubles the spectral efficiency of SEFDM without incurring error penalties. Figure 6 depicts the numerical results of the precoded system with the structure in Fig. 2, showing the substantial BER reduction when compared to the un-coded signal.

V. CONCLUSIONS

This work investigated a new signal processing method to enhance the spectral efficiency of SEFDM systems. We propose a new transceiver structure to generate the new signal format, employing Hilbert pulse pair as shaping pulses. We show that the new system has the major advantage in doubling the spectral efficiency by transmitting two different complex symbols simultaneously and in the same occupied spectrum. Importantly, such doubling of spectral efficiency is achieved without degrading the BER performance. Moreover, the use of turbo coding shows its appropriateness in ameliorating the

BER degradation due to high levels of interference resulting from using SEFDM signal format.

REFERENCES

- [1] M. Rodrigues and I. Darwazeh, "Fast OFDM: A proposal for doubling the data rate of OFDM schemes," 2002.
- [2] 3GPP, "Evolved universal terrestrial radio access (E-UTRA) and evolved universal terrestrial radio access network (E-UTRAN)," 3rd Generation Partnership Project (3GPP), overall description 36.331, Apr 2010, v. 8.12.0.
- [3] A. M. Wyglinski, F. Labeau, and P. Kabal, "Bit loading with BER-constraint for multicarrier systems," *IEEE Transactions on wireless communications*, vol. 4, no. 4, pp. 1383–1387, 2005.
- [4] G. Bansal, J. Hossain, and V. K. Bhargava, "Adaptive power loading for OFDM-based cognitive radio systems," in *Communications, 2007. ICC'07. IEEE International Conference on*. IEEE, 2007, pp. 5137–5142.
- [5] J. B. Anderson, F. Rusek, and V. Öwall, "Faster-than-Nyquist signaling," *Proceedings of the IEEE*, vol. 101, no. 8, pp. 1817–1830, 2013.
- [6] J. E. Mazo, "Faster-than-Nyquist signaling," *Bell System Technical Journal*, vol. 54, no. 8, pp. 1451–1462, 1975.
- [7] M. Rodrigues and I. Darwazeh, "A spectrally efficient frequency division multiplexing based communications system," in *Proc. 8th Int. OFDM Workshop*, 2003, pp. 48–49.
- [8] I. Darwazeh, H. Ghannam, and T. Xu, "The First 15 Years of SEFDM: A Brief Survey," in *2018 11th International Symposium on Communication Systems, Networks & Digital Signal Processing (CSNDSP)*. IEEE, 2018, pp. 1–7.
- [9] D. Rainnie, Y. Feng, and J. Bajcsy, "On capacity merits of spectrally efficient fdm," in *MILCOM 2015-2015 IEEE Military Communications Conference*. IEEE, 2015, pp. 581–586.
- [10] F.-L. Luo and C. Zhang, *Signal processing for 5G: algorithms and implementations*. John Wiley & Sons, 2016.
- [11] R. Gerzaguet, N. Bartzoudis, L. G. Baltar, V. Berg, J.-B. Doré, D. Kténas, O. Font-Bach, X. Mestre, M. Payaró, M. Färber *et al.*, "The 5G candidate waveform race: a comparison of complexity and performance," *EURASIP Journal on Wireless Communications and Networking*, vol. 2017, no. 1, p. 13, 2017.
- [12] P. A. Haigh, P. Chvojka, S. Zvánovec, Z. Ghassemloooy, and I. Darwazeh, "Analysis of Nyquist Pulse Shapes for Carrierless Amplitude and Phase Modulation in Visible Light Communications," *Journal of Lightwave Technology*, vol. 36, no. 20, pp. 5023–5029, 2018.
- [13] S. Isam and I. Darwazeh, "Simple DSP-IDFT techniques for generating spectrally efficient FDM signals," in *Communication Systems Networks and Digital Signal Processing (CSNDSP), 2010 7th International Symposium on*. IEEE, 2010, pp. 20–24.
- [14] A. B. Carlson, *Communication system*. Tata McGraw-Hill Education, 2010.
- [15] A. F. Shalash and K. K. Parhi, "Multidimensional carrierless AM/PM systems for digital subscriber loops," *IEEE Transactions on Communications*, vol. 47, no. 11, pp. 1655–1667, 1999.
- [16] H. Ghannam and I. Darwazeh, "Signal coding and interference cancellation of spectrally efficient FDM systems for 5G cellular networks," in *Telecommunications (ICT), 2017 24th International Conference on*. IEEE, 2017, pp. 1–6.